Synthesis of Arene-Soluble Mixed-Metal Uranium/Zirconium Complexes Using the Dizirconium Nonaisopropoxide Ligand

William J. Evans,* Gregory W. Nyce, Michael A. Greci, and Joseph W. Ziller

Department of Chemistry, University of California, Irvine, California 92697-2025

Received July 3, 2001

The utility of polydentate monoanionic $[Zr_2(O^iPr)_9]^-$ (dzni) in generating arene-soluble, mixed-metal Zr/U complexes is described. $K[Zr_2(O^iPr)_9]$ reacts readily with $UI_3(THF)_4$ to form $[Zr_2(O^iPr)_9]UI_2(THF)$, **1**, in >90% yield. The integrity of the $\{[Zr_2(O^iPr)_9]U\}^{2+}$ unit in **1** was examined by the reaction of **1** with $K_2C_8H_8$, which formed the organometallic complex $[Zr_2(O^iPr)_9]U(C_8H_8)$, **2**. In contrast, the reaction of $K[Zr_2(O^iPr)_9]$ with UCl_4 did not form U(IV)−dzni complexes, and only the ligand exchange product, $[UCl_2(O^iPr)_2(DME)]_2$, **3**, was isolated. The effect of the dzni ligand on the electrochemistry and near-infrared spectroscopy of U(III) is also described.

Introduction

One approach to the disposal of radioactive waste is to embed the radionuclides in inert oxide matrixes that are suitable for long-term storage.[1] Mixed-metal zirconium actinide compounds are of interest in this area of radionuclear waste management since zirconium-based oxides have the proper characteristics to form inert metal oxide matrixes that can hold significant concentrations of decaying elements without major structural failure.[2] For example, $ZrSiO_4$, into which 10 wt % of plutonium has been incorporated, has been shown to be a durable matrix since its radiation-induced crystalline-to-amorphous transition forms an equally inert new phase.[1a] For this type of encapsulation to be successful, the radioactive materials must be homogeneously dispersed in the inert matrix to avoid localized high-intensity radiation damage.

One method to homogeneously distribute radioactive actinides in a zirconium matrix is to prepare zirconium/actinide precursor complexes in which the metals are mixed at the molecular level. Unfortunately, development of syntheses of such complexes is difficult with the highly radioactive elements in the actinide series. However, since trivalent lanthanides and trivalent uranium are the ions most similar in size and chemistry to the transplutonium metals, syntheses of mixed metal zirconium complexes of these metals constitute the best available chemical models.

We have recently been exploring the chemistry of the dizirconium nonaisopropoxide (dzni) ligand[3] with the f elements.[4] This monoanionic polydentate ligand, which often can take the place of the commonly used cyclopentadienyl ligand,[5] has been found to be effective in coordinating, stabilizing, and solubilizing large electropositive elements while providing mixed-metal zirconium-containing compounds. As such, dzni could provide an effective way to make mixed zirconium/actinide complexes, a class of molecules for which no crystallographically characterized examples are reported in the literature to our knowledge. We report here the first chemistry of the dzni ligand with uranium.

Experimental Section

The chemistry described below was performed under nitrogen or argon with rigorous exclusion of air and water by using Schlenk, vacuum line, and glovebox techniques. Solvents were purified as previously described.[6] $K[Zr_2(O^iPr)_9]$,[3b] $UI_3(THF)_4$,[7] $K_2C_8H_8$,[8] and UCl_4[9] were prepared according to literature procedures. NMR spectra and magnetic moments, measured by the method of Evans,[10] were recorded using a Bruker DRX400 spectrometer at 298 K. All magnetic data were obtained in C_6H_6. Infrared spectra for **1** and **2** were recorded as thin films on a ASI ReactIR 1000 instrument. The infrared spectrum for **3** was recorded from KBr pellet on a Perkin-Elmer 283 IR spectrometer. The vis/near-IR spectra were recorded on a Perkin-Elmer Lambda 900 UV/VIS/NIR spectrophotometer using 1 cm quartz cells. All spectra were obtained using a solvent reference blank. Electrochemical studies were performed in an inert-atmosphere drybox with a Princeton

(1) (a) Ewing, R. C.; Lutze, W.; Weber, W. J. *J. Mater. Res*. **1995**, *10*, 243. (b) Ewing, R. C.; Weber, W. J.; Clinard, F. W. *Prog. Nucl. Energy* **1995**, *29*, 63. (c) Clinard, F. W., Jr.; Hurley, G. F.; Hobbs, L. W. *J. Nucl. Mater*. **1982**, *108/109*, 655.

(2) (a) Weber, W. J. *Radiat. Eff*. **1983**, *77*, 295. (b) Clinard, F. W., Jr.; Rohr, D. L.; Roof, R. B. *Nucl. Instrum. Methods Phys. Res. B* **1984**, *1*, 581.

(3) (a) Vaarstra, B. A.; Huffman, J. C.; Streib, W. E.; Caulton, K. G. *J. Chem. Soc., Chem. Commun*. **1990**, 1750. (b) Vaarstra, B. A.; Streib, W. E.; Caulton, K. G. *J. Am. Chem. Soc*. **1990**, *112*, 8593. (c) Vaarstra, B. A.; Huffman, J. C.; Streib, W. E.; Caulton, K. G. *Inorg. Chem*. **1991**, *30*, 3068. (d) Vaarstra, B. A.; Samuels, J. A.; Barash, E. H.; Martin, J. D.; Streib, W. E.; Gasser, C.; Caulton, K. G. *J. Organomet. Chem*. **1993**, *449*, 191. (e) Samuels, J. A.; Chiang, W. C.; Huffman, J. C.; Trojan, K. L.; Hatfield, W. E.; Baxter, D. V.; Caulton, K. G. *Inorg. Chem*. **1994**, *33*, 2167. (f) Teff, T. J.; Huffman, J. C.; Caulton, K. G. *Inorg. Chem*. **1995**, *34*, 2491. (g) Sogani, S.; Singh, A.; Bohra, R.; Mehrotra, R. C.; Noltemeyer, M. *J. Chem. Soc., Chem. Commun*. **1991**, 738. (h) Veith, M.; Mathur, S.; Huch, V. *J. Am. Chem. Soc*. **1996**, *118*, 903. (i) Veith, M.; Mathur, S.; Huch, V. *J. Chem. Soc., Dalton Trans*. **1996**, 2485. (j) Garg, G.; Singh, A.; Mehrotra, R. C. *Polyhedron* **1993**, *12*, 1399. (k) Singh, A.; Mehrotra, R. C. *Polyhedron* **1998**, *17*, 689.

(4) (a) Evans, W. J.; Greci, M. A.; Johnston, M. A.; Ziller, J. W. *Chem. Eur. J*. **1999**, *5*, 3482. (b) Evans, W. J.; Johnston, M. A.; Greci, M. A.; Ansari, M. A.; Brady, J. C.; Ziller, J. W. *Inorg. Chem*. **2000**, *39*, 2125. (c) Evans, W. J.; Greci, M. A.; Ansari, M. A.; Ziller, J. W. *J. Chem. Soc., Dalton Trans*. **1997**, *23*, 4503.

(5) Evans, W. J.; Greci, M. A.; Ansari, M. A.; Ziller, J. W. *J. Chem. Soc., Dalton. Trans*. **1997**, *23*, 4503.

(6) Evans, W. J.; Chamberlain, L. R.; Ulibarri, T. A.; Ziller, J. W. *J. Am. Chem. Soc*. **1988**, *110*, 6423.

(7) Avens, L. R.; Bott, S. G.; Clark, D. L.; Sattelberger, A. P.; Watkin, J. G.; Zwick, B. D. *Inorg. Chem*. **1994**, *33*, 2248.

(8) Katz, T. J. *J. Am. Chem. Soc*. **1960**, *82*, 3784.

(9) Sherill, H. J.; Durret, D. G.; Selbin, J. *Inorg. Synth*. **1974**, *15*, 243.

(10) Evans, D. F. *J. Chem. Soc*. **1959**, 2003. Becconsall, J. K. *Mol. Phys*. **1968**, 15, 129.

10.1021/ic010703x CCC: $20.00
Published on Web 11/20/2001

Research Model 273A electrochemical system in THF using a saturated solution of $[Bu_4N][PF_6]$ as the supporting electrolyte and a glassy carbon working electrode, platinum wire counter electrode, and Ag/AgCl reference electrode. Oxidations of **1** and **2** were irreversible at scan speeds ranging from 1 V s^{-1} to 50 mV s^{-1}. Elemental analyses were performed by Analytische Laboratorien, Lindlar, Germany.

$[Zr_2(O^iPr)_9]UI_2(THF)$, 1. In a glovebox, a solution of $KZr_2(O^iPr)_9$ (83 mg, 0.11 mmol) in 5 mL of toluene was added to a stirred purple solution of $UI_3(THF)_4$ (100 mg, 0.11 mmol) in 5 mL of toluene. After 6 h the red-purple solution was centrifuged to remove a white precipitate. The supernatant was dried by rotary evaporation to yield **1** (135 mg, 96%) as a dark purple powder. Crystals suitable for X-ray diffraction were grown by cooling a saturated toluene/THF (10:1) solution of **1** to −30 °C. ^{1}H NMR (C_6D_6): δ −15.5 (s br, 12H, OCH(CH_3)$_2$), −4.5 (s br, 12H, OCH(CH_3)$_2$), −3.7 (s br, 2H, OC*H*(CH_3)$_2$), 2.1 (s 4H, THF), 2.2 (d, 12H, OCH(CH_3)$_2$), 3.0 (d, 12H, OCH(CH_3)$_2$), 6.2 (s, 4H, THF), 7.0 (s br, 2H, OC*H*(CH_3)$_2$), 7.4 (d, 6H, OCH(CH_3)$_2$), 10.3 (s br, 2H, OC*H*(CH_3)$_2$), 13.3 (sept, 1H, OC*H*(CH_3)$_2$). IR: 2968 s, 2930 m, 2868 m, 2629 w, 1463 m 1366 m, 1339 w, 1262 w, 1166 s, 1127 s 1004 s, 945 s, 919 s, 849 m, 830 m, 803 m, 679 m cm^{-1}. Vis/near-IR [(toluene, λ_{max}, nm (ϵ, M^{-1} cm^{-1})]: 435(700), 502(890), 510(880), 536(800), 610(580), 644(620), 654(620), 734(150), 812(10) 860(50), 872(50), 917(75), 947(20), 1007(60), 1037(30), 1072(30), 1168(15), 1221(20), 1243(30). Magnetic susceptibility: $\chi_g^{298\ K} = 2.6 \times 10^{-6}$, $\mu_{eff}^{298\ K} = 2.8\ \mu_B$. Anal. Calcd for $C_{31}H_{71}O_{10}I_2Zr_2U$: C, 29.52; H, 5.62. Found C, 29.71; H, 5.37.

$[Zr_2(O^iPr)_9]U(C_8H_8)$, 2. In a glovebox, a dark purple toluene solution of **1** (200 mg, 0.15 mmol) was added to a toluene slurry of $K_2C_8H_8$ (29 mg, 0.15 mmol). After 6 h the dark green solution was centrifuged to remove a white precipitate and a small quantity of green precipitate that has properties consistent with $(C_8H_8)_2U$. The supernatant was dried by rotary evaporation to yield **2** (132 mg, 80%) as a forest green powder. Crystals suitable for X-ray diffraction were grown by cooling a saturated hexanes solution of **2** to −30 °C. ^{1}H NMR (C_6D_6): δ −39.8 (s, 8H, C_8H_8), −24.8 (s br, 12H, OCH(CH_3)$_2$), 0.0 (s br, 12H, OCH(CH_3)$_2$), 3.0 (s br, 12H, OCH(CH_3)$_2$), 3.3 (s br, 12H, OCH(CH_3)$_2$), 6.3 (s br, 2H, OC*H*(CH_3)$_2$), 7.6 (s br, 6H, OCH(CH_3)$_2$), 8.0 (s br, 2H, OC*H*(CH_3)$_2$), IR: 3038 m, 2968 s, 2930 m, 2868 m, 2629 w, 1478 m 1378 m, 1336 w, 1231 w, 1166 s, 1131 s 1007 s, 953 s, 930 s, 845 m, 810 m, 706 m, 675 m cm^{-1}. VIS/near-IR [(toluene, λ_{max}, nm (ϵ, M^{-1} cm^{-1})] 447(950), 540(350), 560(340), 596(410), 615(420), 698(300), 822(400), 900(170), 930(200), 991(110), 1043(140), 1120(120), 1158(90), 1248(70). Magnetic susceptibility: $\chi_g^{298\ K} = 2.8 \times 10^{-6}$, $\mu_{eff}^{298\ K} = 2.6\ \mu_B$. Anal. Calcd for $C_{35}H_{71}O_9Zr_2U$: C, 39.79; H, 6.77. Found C, 37.94; H, 6.57.

$[UCl_2(O^iPr)_2(DME)]_2$, 3. In a glovebox, UCl_4 (318 mg, 0.838 mmol) and $KZr_2(O^iPr)_9$ (631 mg, 0.838 mmol) were combined in 10 mL of THF. The light green solution changed to light purple within 30 min with formation of a light purple precipitate. The reaction mixture was stirred for 8 h. The solvent was removed by rotary evaporation. The crude reaction mixture was extracted with 10 mL of DME to yield a light purple solution. The volume was reduced to 2 mL by rotary evaporation, and purple crystals were obtained at −30 °C (93 mg, 26% (based on UCl_4)). IR (KBr): 2965 s, 2926 m, 2878 m, 1734 w, 1623 w, 1459 m, 1367 m, 1328 w, 1294 w, 1256 m, 1198 w, 1125 s, 1087 m, 1036 m, 1034 m, 980 s, 922 w, 860 m, 840 m, 811 w, 739 w, 695 w, 667 w, 594 w, 541 w cm^{-1}. Anal. Calcd. for $C_{20}H_{48}O_8Cl_4U_2$: C, 23.22; H, 4.68; U, 46.02. Found: C, 23.31; H, 4.82; U, 46.70.

X-ray Data, Collection, Structure Determination, and Refinement for 1. A dark red-purple crystal of approximate dimensions 0.18 × 0.22 × 0.25 mm was mounted on a glass fiber and transferred to a Bruker CCD platform diffractometer. The SMART[11] program package was used to determine the unit-cell parameters and for data collection (30 s/frame scan time for a sphere of diffraction data). The raw frame data were processed using SAINT[12] and SADABS[13] to yield the reflection data files. Subsequent calculations were carried out using the SHELXTL[14] program. The diffraction symmetry was 2/*m*, and the systematic absences were consistent with the centrosymmetric monoclinic space group $P2_1/n$, which was later determined to be correct.

Table 1. Data Collection Parameters[a] for $[Zr_2(O^iPr)_9]UI_2(THF)$, **1**, $[Zr_2(O^iPr)_9]U(C_8H_8)$, **2**, and $[UCl_2(O^iPr)_2(DME)]_2$, **3**

	1	**2**	**3**
formula	$C_{33}H_{73}I_2O_{10}UZr_2$	$C_{70}H_{142}O_{18}U_2Zr_4$	$C_{20}H_{48}Cl_4O_8U_2$
fw	1314.20	1056.39	1034.44
temp (K)	158	158	163
cryst syst	monoclinic	triclinic	monoclinic
space group	$P2_1/n$	$P\bar{1}$	$C2/c$
a (Å)	12.5451(11)	12.6047(7)	19.041(4)
b (Å)	21.4149(19)	20.2204(12)	11.9606(12)
c (Å)	18.2977(16)	20.3064(12)	15.4779(14)
α (deg)	90	117.0350(10)	90
β (deg)	104.252(2)	95.3300(10)	108.990(9)
γ (deg)	90	105.0840(10)	90
V (Å^3)	4764.4(7)	4314.9(4)	3333.1(8)
Z	4	2	4
ρ_{calcd} (mg/m^3)	1.829	1.626	2.061
μ (mM^{-1})	5.160	4.262	10.061
R1, $I > 2.0\sigma(I)$	0.0314	0.0481	0.0333
wR2 (all data)	0.0623	0.1237	0.0879

[a] Radiation: Mo Kα (μ = 0.71073 Å). Monochromator: highly oriented graphite. $R1 = \sum||F_o| - |F_c||/\sum|F_c|$; $wR2 = [\sum[w(F_o^2 - F_c^2)^2/\sum[w(F_o^2)^2]]^{1/2}$.

Table 2. Selected Bond Distances (Å) and Angles (deg) for $[Zr_2(O^iPr)_9]UI_2(THF)$, **1**

U(1)−I(1)	3.1150(4)	U(1)−I(2)	3.1563(4)
U(1)−O(10)	2.595(3)	U(1)−O(1)	2.612(3)
U(1)−O(2)	2.498(2)	U(1)−O(3)	2.480(3)
U(1)−O(4)	2.425(3)	U(1)···Zr(1)	3.5899(5)
U(1)···Zr(2)	3.5639(5)	Zr(1)···Zr(2)	3.3481(6)
O(4)−U(1)−O(3)	125.18(10)	O(4)−U(1)−O(2)	69.78(9)
O(4)−U(1)−O(1)	63.89(9)	I(1)−U(1)−I(2)	102.113(11)
Zr(1)−U(1)−Zr(2)	55.809(11)	O(10)−U(1)−I(1)	82.72(7)
O(10)−U(1)−I(2)	78.77(7)		

The structures were solved by direct methods and refined on F^2 by full matrix least-squares techniques. The analytical scattering factors[15] for neutral atoms were used throughout the analysis. Carbon atom (C25) was disordered and included using multiple components with partial site-occupancy factors. There was one-half molecule of THF solvent molecule present per formula unit. The solvent was disordered and included as above. Hydrogen atoms were included using a riding model. The hydrogen atoms associated with the THF solvent molecule were not included. At convergence, wR2 = 0.0623 and GOF = 1.007 for 432 variables refined against 9715 data (0.80 Å resolution). As a comparison for refinement on *F*, R1 = 0.0314 for those 8039 data with $I > 2.0\sigma(I)$. Experimental parameters for the data collection and structure refinement for **1** are given in Table 1. Selected bond distances are give in Table 2.

X-ray Data, Collection, Structure Determination, and Refinement for 2. A dark green crystal of approximate dimensions 0.22 × 0.38 × 0.45 mm was mounted on a glass fiber and transferred to a Bruker CCD platform diffractometer. The SMART[11] program package was used to determine the unit-cell parameters and for data collection (20 s/frame scan time for a sphere of diffraction data). The raw frame data were processed using SAINT[12] and SADABS[13] to yield the reflection data files. Subsequent calculations were carried out using the SHELXTL[14] program. There were no systematic absences and no diffraction symmetry other than the Friedel condition. The centrosymmetric triclinic space group $P\bar{1}$ was assigned and later determined to be correct.

The structures were solved by direct methods and refined on F^2 by full matrix least-squares techniques. The analytical scattering factors[15]

(11) *SMART Software Users Guide*, version 4.21; Bruker Analytical Systems X-ray Systems, Inc.: Madison, WI, 1997.
(12) *SAINT Software Users Guide*, version 4.05; Bruker Analytical X-ray Systems, Inc.: Madison, WI, 1997.
(13) Sheldrick, G. M. *SADABS*; Bruker Analytical X-ray Systems, Inc.: Madison, WI, 1997.
(14) Sheldrick, G. M. *SHELXTL*, version 5.10; Bruker Analytical X-ray Systems, Inc.: Madison, WI, 1997.
(15) *International Tables for X-ray Crystallography*; Kluwer Academic Publishers: Dordrecht, 1992; Vol. C.

Table 3. Selected Bond Distances (Å) and Angles (deg) for $[Zr_2(O^iPr)_9]U(C_8H_8)$, **2**

U(1)−C(34)	2.711(7)	U(1)−C(30)	2.722(7)
U(1)−C(35)	2.728(7)	U(1)−C(33)	2.730(8)
U(1)−C(31)	2.737(7)	U(1)−C(29)	2.749(7)
U(1)−C(32)	2.750(8)	U(1)−C(28)	2.759(7)
U(1)−Cnt(1)	2.029	U(1)−O(1)	2.612(4)
U(1)−O(2)	2.621(4)	U(1)−O(3)	2.563(4)
U(1)−O(4)	2.589(4)	U(1)−Zr(1)	3.6399(6)
U(1)−Zr(2)	3.6440(7)	Zr(1)−Zr(2)	3.3219(9)
O(4)−U(1)−O(3)	57.80(13)	O(4)−U(1)−O(2)	64.74(13)
O(4)−U(1)−O(1)	64.44(14)	O(1)−U(1)−O(2)	122.11(13)
Zr(1)−U(1)−Zr(2)	62.803(15)		

for neutral atoms were used throughout the analysis. There are two molecules in the formula unit. The carbon atoms of the isopropyl groups defined by C(16)−C(18) and C(57)−C(59) were disordered. Those atoms were included using multiple components with partial site-occupancy factors. Hydrogen atoms were included using a riding model. At convergence, wR2 = 0.1237 and GOF = 1.028 for 841 variables refined against 17 543 data (0.80 Å resolution). As a comparison for refinement on *F*, R1 = 0.0481 for those 14 001 data with $I > 2.0\sigma(I)$. Experimental parameters for the data collection and structure refinement for **2** are given in Table 1. Selected bond distances are given in Table 3.

X-ray Data Collection and Solution and Refinement for 3. A violet crystal was coated with Paratone oil, mounted on glass fibers, and transferred to a Siemens P4 diffractometer. The XSCANS program package[16] determinations of symmetry, crystal class, unit-cell parameters, and the crystal's orientation matrix were carried out according to standard procedures. Intensity data were collected at 163 K using the $2\theta/\omega$ scan technique with Mo Kα radiation. The raw data were processed with a local version of CARESS,[17] which employs a modified version of the Lehman−Larsen algorithm to obtain intensities and standard deviations from the measured 96-step peak profiles. Subsequent calculations were carried out using the SHELXTL[18] program. All data were corrected for absorption and for Lorentz and polarization effects and placed on an approximately absolute scale. The diffraction symmetry was 2/*m* and the systematic absences were consistent with space groups *Cc* and *C*2/*c*. It was later determined that the centrosymmetric monoclinic space group *C*2/*c* was correct.

The structure was solved by direct methods and refined on F^2 by full-matrix least-squares techniques. The analytical scattering factors[15] for neutral atoms were used throughout the analysis. The molecule was a dimer and located about an inversion center. The carbon atoms of the isopropyl ligands were disordered. These atoms were included using multiple components with partial site-occupancy factors. Hydrogen atoms were included using a riding model. At convergence, wR2 = 0.0879 and GOF = 1.042 for 149 variables refined against all 2949 unique data. As a comparison for refinement of *F*, R1 = 0.0333 for those 2429 data with $I > 2.0\sigma(I)$). Experimental parameters for the data collection and structure refinement for **3** are given in Table 1. Selected bond distances and angles for **3** are given in Table 4.

Results and Discussion

Synthesis of $[Zr_2(O^iPr)_9]UI_2(THF)$, 1. $UI_3(THF)_4$ reacts readily with $KZr_2(O^iPr)_9$ to form $[Zr_2(O^iPr)_9]UI_2(THF)$, **1**, in high yield, eq 1.

$$KZr_2(O^iPr)_9 + UI_3(THF)_4 \xrightarrow[-3THF]{-KI} \underset{\mathbf{1}}{[Zr_2(O^iPr)_9]UI_2(THF)} \quad (1)$$

Initially, THF was used as a solvent, but this consistently formed oily products that yielded **1** as a red-purple powder only after repeated trituration in hexanes. Subsequently, toluene was found to be a better solvent, since **1** can be directly obtained in powder form. Complex **1** is soluble in THF, moderately soluble in toluene, and insoluble in hexanes.

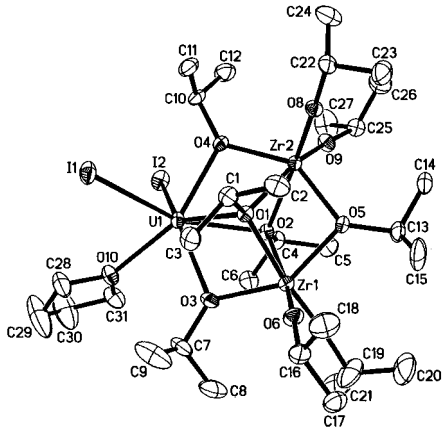

Figure 1. Plot of $[Zr_2(O^iPr)_9]UI_2(THF)$, **1**, with thermal ellipsoids drawn at the 50% probability level.

Table 4. Selected Bond Distances (Å) and Angles (deg) for $[UCl_2(O^iPr)_2(DME)]_2$, **3**

U−O(1)	2.052(5)	U−O(2)	2.055(5)
U−Cl(1)	2.8189(18)	U−Cl(2)	2.6892(19)
U−O(3)	2.548(5)	U−O(4)	2.620(5)
U−Cl(1_)	2.8442(18)		
O(1)−U−O(2)	178.3(2)	O(1)−U−Cl(2)	91.05(18)
O(2)−U−Cl(2)	87.99(17)	O(1)−U−Cl(1)	91.12(16)
Cl(2)−U−Cl(1)	80.12(5)	Cl(1)−U−Cl(1′)	72.49(6)
Cl(2)−U−O(3)	76.83(13)	O(1)−U−O(3)	79.9(2)
O(3)−U−O(4)	63.23(16)	O(1)−U−O(4)	102.1(2)
O(4)−U−Cl(1_)	74.05(12)	O(2)−U−O(3)	98.4(2)
O(2)−U−O(4)	77.61(19)		

Although **1** is paramagnetic, it can be studied by NMR spectroscopy. The ^{1}H NMR spectrum of **1** in C_6D_6 displays five separate chemical shifts in a 2:2:2:2:1 ratio that can be assigned to the methyl groups of the isopropoxide ligands. This pattern is similar to that found in previously characterized $[Zr_2(O^iPr)_9]^-$-containing complexes.[3b] The methine resonances were more difficult to observe, and only four of the five expected signals were identified. X-ray crystallography was employed to definitively characterize **1** (Figure 1).

Synthesis of $[Zr_2(O^iPr)_9]U(C_8H_8)$, 2. To determine if the dzni−U^{III} unit would remain intact in subsequent reactions, the reaction of **1** with $K_2C_8H_8$ was examined. **1** was found to react with $K_2C_8H_8$ in toluene to form **2** as a dark green powder in good yield, eq 2.

$$\underset{\mathbf{1}}{[Zr_2(O^iPr)_9]UI_2(THF)} + K_2C_8H_8 \xrightarrow[-THF]{-2KI} \underset{\mathbf{2}}{[Zr_2(O^iPr)_9]U(C_8H_8)} \quad (2)$$

As in the synthesis of **1**, toluene proved to be a better solvent than THF to yield **2** as a tractable product. The ^{1}H NMR spectrum of **2** contains five separate resonances for the methyl groups of the isopropoxide ligands in a 2:2:2:2:1 ratio and a single resonance for the $C_8H_8^{2-}$ ligand at −39.8 ppm. As in the case of **1**, not all of the methine resonances were observed. X-ray crystallography was employed to definitively characterize **2** (Figure 2). **2** represents one of the few U(III)/$C_8H_8^{2-}$ complexes reported in the literature.[19]

(16) XSCANS Software Users Guide, Version 2.1, Siemens Analytical X-ray Systems, Inc.; Madison, WI, 1994.
(17) Broach, R. W. Argonne National Laboratory, IL, 1978.
(18) Sheldrick, G. M.; Siemens Analytical X-ray Instruments, Inc.; Madison, WI, 1994.

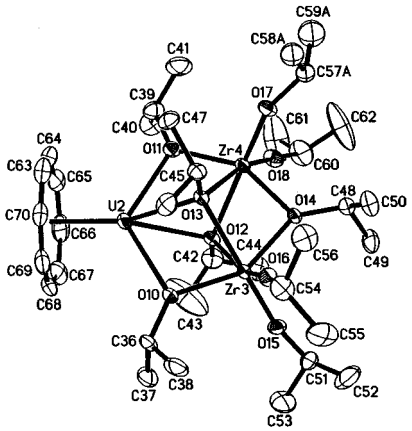

Figure 2. Plot of $[Zr_2(O^iPr)_9]U(C_8H_8)$, **2**, with thermal ellipsoids drawn at the 30% probability level.

Structural Studies of 1 and 2. In both **1** and **2**, the $[Zr_2(O^iPr)_9]^-$ unit coordinates to U(III) as a tetradentate ligand through two triply bridging and two doubling bridging isopropoxide oxygen atoms. This is the typical coordination mode found for this metalloalkoxide ligand in previously characterized dzni lanthanide complexes.[4] The additional two iodide ligands and THF give the uranium in **1** a formal coordination number of seven. This is similar to that of the trivalent lanthanide ions in the $\{[Zr_2(O^iPr)_9]LnCl(\mu\text{-}Cl)\}_2$ (Ln = Ce, Nd) series[4b,c] except that in **1** none of the ligands are bridging and a monomeric complex is observed in the solid state. The coordination environment of **2** is similar to that in $[Zr_2(O^iPr)_9]Sm(C_8H_8)$,[4a] although the two complexes are not isomorphous.

In **1**, the 3.1150(4) Å U−I(1) and 3.1559(4) Å U−I(2) distances are similar to the 3.13(2) Å average U−I distance in $UI_3(THF)_4$.[7] The 2.596(3) Å U−O(THF) is longer than the 2.52(1) Å length found in $UI_3(THF)_4$, presumably because the steric bulk of the $[Zr_2(O^iPr)_9]^-$ ligand is greater than that of the $[(THF)_3I]^-$ ligand set in $UI_3(THF)_4$. As shown in Table 2, the U−O(μ_3-O^{i}Pr) distances in **1** are longer than the U−O(μ_2-O^{i}Pr) lengths as is typical in other f element dzni complexes. Another similarity with other f element dzni systems[4,5] is that the two U−O(μ_2-O^{i}Pr) distances have more similar values than the two U−O(μ_3-O^{i}Pr) distances. In **1**, the 2.496(2) and 2.610(3) U−O(μ_3-O^{i}Pr) values are particularly disparate, which suggests that the dzni ligand can adjust to asymmetrical ligand arrangements on the opposite side of the complex. In this case, the longest U−O(μ_3-O^{i}Pr) bond is on the same side as the largest ligand, iodide. Comparison of **1** with $(C_5Me_5)UI_2(THF)_3$[20] provides another example in f element chemistry where the dzni ligand can replace the $[(C_5Me_5)(THF)_2]^-$ ligand set.[5]

In **2**, the 2.564(4)−2.621(4) Å U−O distances are larger than those in **1**, which is consistent with the higher formal coordination number of **2** generated by the $(C_8H_8)^{2-}$ versus $[I_2(THF)]^{2-}$ ligand set. The 2.743(7) Å average U−C(C_8H_8) distance in **2** is similar to those found in the only three other structurally characterized U^{III}−(C_8H_8) complexes, $(C_8H_8)(C_5Me_5)U$(4,4'-dimethyl-2,2'-bipyridine),[19a] $[K(diglyme)][U(C_8H_7Me)_2]$,[19b] and $[(C_8H_8)U(HMPA)_3][BPh_4]$,[19c] in which the average distances are 2.703, 2.707(7), and 2.71(4) Å, respectively. This suggests that the dzni ligand is sterically equivalent to the $[(C_5Me_5)(Me_2bpy)]^-$ and $[(C_8H_7Me)K(diglyme)]^-$ ligand sets. This is consistent with previous f element studies that suggest that $[Zr_2(O^iPr)_9]^-$ is larger than $[C_5Me_5]^-$.[4c]

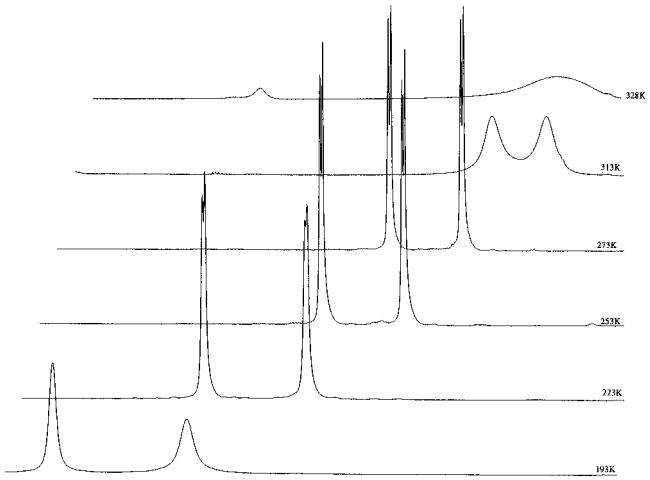

Figure 3. Variable temperature ^{1}H NMR of two O^{i}Pr signals in compound **2**.

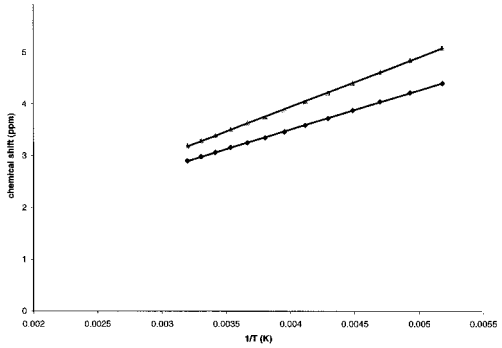

Figure 4. Temperature dependence of ^{1}H NMR shifts of two O^{i}Pr signals in compound **2**.

Solution Dynamics of $[Zr_2(O^iPr)_9]U(C_8H_8)$, 2. The dzni ligand in **2** exhibits fluxional behavior in solution. Coalescence of two isopropyl signals in the ^{1}H NMR spectrum occurs at 55 °C (Figure 3). Due to the paramagnetism of U(III), the ^{1}H NMR shifts are temperature dependent, but the shifts are linear with respect to T^{-1} (Figure 4). The barrier for this fluxional process ($\Delta G^{\ddagger}$ = 15.7 kcal/mol) was calculated using chemical shifts extrapolated from the coalescence temperature.[21] No fluxional process was observed for compound **1** up to 110 °C.

Electrochemistry. Cyclic voltammetry on **1** and **2** in THF gave irreversible oxidation waves at $E_{pa} = -0.8$ and -1.5 V, respectively (vs a ferrocene/ferrocenium internal standard).[22] Variation of scan rates had little effect on the potential values, and no evidence for reversiblility was observed. The more negative value for compound **2** versus **1** is likely due to the greater electron-donating ability of the $C_8H_8^{2-}$ ligand compared to iodide. The oxidation potentials of **1** and **2** are comparable to the few U(III) values reported in the literature. $(C_8H_8)(C_5Me_5)U$(4,4'-dimethyl-2,2'-bipyridine) has a reported redox potential of −0.69 V vs SHE (−1.1 V vs ferrocene).[19a] $U[N(SiMe_3)_2]_3$ and $U(OAr)_3$ (OAr = 2,6-di-*tert*-butylphenoxide) were reported to exhibit reversible oxidation waves of $E_{1/2}$ =

(19) (a) Schake, A. R.; Avens, L. R.; Burns, C. J.; Clark, D. L.; Sattelburger, A. P.; Smith, W. H. *Organometallics* **1993**, *12*, 1497. (b) Boussie, T. R.; Eisenberg, D. C.; Rigsbee, J. Streitweiser, A.; Zalkin, A. *Organometallics*, **1991**, *10*, 1922. (c) Cendrowski-Guillaume, S. M.; Nierlich, M.; Ephritikhine, M. *Eur. J. Inorg. Chem*. **2001**, 1495.

(20) Avens, L. R.; Burns, C. J.; Butcher, R. J.; Clark, D. L.; Gordon, J. C.; Schake, A. R.; Scott, B. L.; Watkin, J. G.; Zwick, B. D. *Organometallics* **2000**, *19*, 451.

(21) (a) Luke, W. D.; Streitweiser, A., Jr. *J. Am. Chem. Soc*. **1981**, *103*, 3241. (b) Sandström, J. *Dynamic NMR Spectroscopy*; Academic Press: London, 1982. (c) Lukens, W. W., Jr.; Beshouri, S. M.; Stuart, A. L.; Andersen, R. A. *Organometallics* **1999**, *18*, 1247.

(22) Connelly, N. G.; Geiger, W. E. *Chem. Rev*. **1996**, *96*, 877.

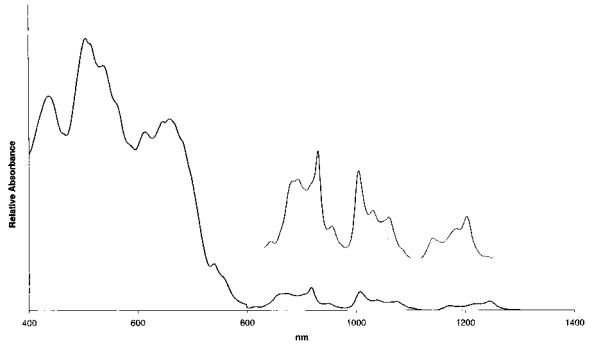

Figure 5. Visible/near-IR spectrum of $[Zr_2(O^iPr)_9]UI_2(THF)$, **1**.

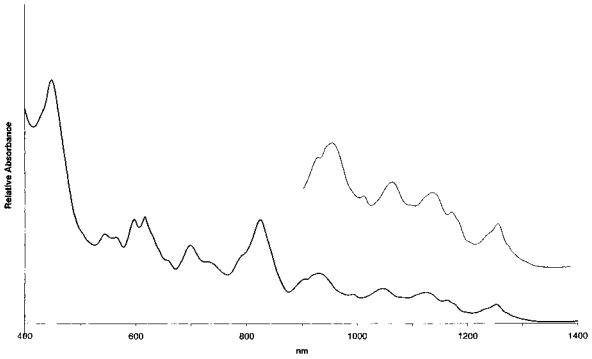

Figure 6. Visible/near-IR spectrum of $[Zr_2(O^iPr)_9]U(C_8H_8)$, **2**.

−1.24 and −1.22 V, respectively (vs a ferrocene/ferrocenium internal standard).[23] $(C_5Me_5)_2UCl(THF)$ is reported to undergo a single oxidation wave in THF at $E_{pa} = -0.71$ V vs SCE (−1.27 V vs ferrocene).[24]

Electronic Absorption Spectroscopy. The room-temperature electronic absorption spectra of **1** and **2** were recorded in toluene solutions. The strong absorption bands at 436, 501, 612, and 644 nm (ϵ =600−900 M^{-1} cm^{-1}) found for **1** are similar to those reported for $UI_3(THF)_4$.[7] In **2**, the most intense absorption band was observed at 447 nm (ϵ = 950 M^{-1} cm^{-1}) and strong absorptions were also found in the 540−830 nm (ϵ = 300−420 M^{-1} cm^{-1}) region. As shown in Figure 5, the NIR spectrum (800−1400 nm) of **1** has similar features to the spectra reported for $UI_3(THF)_4$7 and U(III) aquo ion in perchloric acid.[25] However, substitution of the iodide ligands in **1** with a $(C_8H_8)^{2-}$ ligand in **2** changes the NIR spectrum (Figure 6).[26] The position and the weak intensity of the absorptions in the 800−1400 nm region for **1** (ϵ = 10−80 M^{-1} cm^{-1}) and **2** (ϵ = 70−200 M^{-1} cm^{-1}) have been attributed to Laporte forbidden f→f transitions of the U(III) center.[7]

UCl_4 Reactions. In addition to the U(III) chemistry described above, attempts to synthesize dzni−U(IV) complexes were made under a variety of conditions. Reaction of the dzni potassium precursor, $KZr_2(O^iPr)_9$, with UCl_4 did not yield a $[Zr_2(O^iPr)_9]$-UCl_3 product. Instead only the ligand redistribution product, $[UCl_2(O^iPr)_2(DME)]_2$, **3**, was isolated in low yield**.** Since the ^1H NMR spectrum was uninformative, this complex was characterized by X-ray crystallography (Figure 7). Attempts to synthsize a U(IV)−dzni complex by oxidizing **1** were also

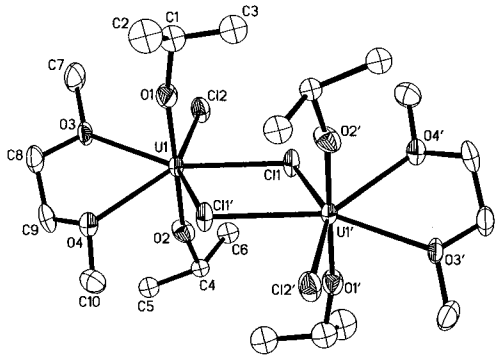

Figure 7. Plot of $[UCl_2(O^iPr)_2(DME)]_2$, **3**, with thermal ellipsoids drawn at the 50% probability level.

unsuccessful. Oxidation of **1** with HgI_2 did not lead to an isolable U(IV)−dzni compound.

The structure of **3** can be compared with several bimetallic U(IV) isopropoxide complexes in the literature including $U_2(O^iPr)_{10}$,[27] $U_2I_4(O^iPr)_4(HO^iPr)_2$,[28] $U_2(\eta^3\text{-}C_3H_5)_4(O^iPr)_4$,[29] and $U_2(C_8H_8)_2(O^iPr)_4$.[30] However, complex **3** differs from these complexes in that the choride ligands bridge the two uranium atoms rather than the isopropoxide ligands, which are the bridging ligands in the other examples. Each uranium in **3** has a distorted pentagonal bipyramidal coordination geometry with the isopropoxide ligands in the axial positions. The O(1)−U−O(2) angle is 178.3(2)° and the [O−(axial)]−U−Cl angles are near the expected 90°. However, the [O(axial)]−U−[O(DME)] angles show that one of the DME oxygens is above and one is below the pentagonal plane of the pentagonal bipyramid: O(1)−U(1)−O(3), 79.9(2)°; O(1)−U(1)−O(4), 102.1(2)°. The angles between the donor atoms in the plane are irregular, since the DME ligand is a chelate and two of the chlorides are bridging (they are effectively part of a metallochelate). The U−O(isopropoxide) distances are comparable to the terminal isopropoxide U−O distances in the four complexes cited above.

3 is also similar to the structure of $[UCl_3(\mu\text{-}Cl)THF_2]_2$,[31] **4**, with replacement of the axial chlorides with isopropoxides and the two THF ligands with DME. The bridging U−Cl distances are very similar to the 2.792(3) and 2.916(3) Å values in **4**. The terminal 2.6892(19) Å U−Cl distance in **3** is longer than the 2.600(3) Å analogue in **4**, as are the U−O(DME) distances in **4**. The 2.8189(8) Å terminal U−Cl distance in **3** is also longer than those in $UCl_4(THF)_3$,[32] 2.592(2) Å, and $(C_5Me_5)_2UCl_2$,[33] 2.583(6) Å.

Conclusions

The ionic metathesis reaction of $K[Zr_2(O^iPr)_9]$ with $UI_3(THF)_4$ is a convenient way to make arene-soluble mixed-metal Zr/U compounds **1** and **2**. The high yield synthesis of **2** from **1** is consistent with the ability of the $[Zr_2(O^iPr)_9]^-$ ligand to maintain its structural integrity during organometallic reactions. In

(23) Avens, L. R.; Barnhart, D. M.; Burns, C. J.; McKee, S. D.; Smith, W. H. *Inorg. Chem*. **1994**, *33*, 4245.
(24) Finke, R. G.; Gaughan, G.; Voegeli, R. *J. Organomet. Chem*. **1982**, *229*, 179.
(25) Cohen, D.; Carnall, W. T. *J. Phys. Chem*. **1960**, *64*, 1933.
(26) $K_2(C_8H_8)$ has no measurable absorptions in the near-IR region from 2000 to 800 nm.
(27) Cotton, F. A.; Morler, D. O.; Schwotzer, W. *Inorg. Chem. Acta* **1985**, *85*, LC31.
(28) Van der Sluys, W. G.; Huffman, J. C.; Ehler, D. S.; Sauer, N. N. *Inorg. Chem*. **1992**, *31*, 1316.
(29) Brunelli, M.; Perengo, C.; Lugili, G.; Mazzei, A. *J. Chem. Soc., Dalton. Trans*. **1979**, 861.
(30) Arliguie, T.; Baudry, D.; Ephritikhine, M.; Nierlich, M.; Lance, M.; Vigner, J. *J. Chem. Soc., Dalton Trans*. **1992**, 1019.
(31) Rebizant, J.; Spirlet, M. R.; Apostolidis, C.; Van Den Bossche, G.; Kanellakopulos, B. *Acta Crystallogr*. **1991**, *C47*, 864.
(32) Van Der Sluys, W. G.; Berg, J. M.; Barnhardt, D.; Sauer, N. N. *Inorg. Chim. Acta* **1993**, *204*, 251.
(33) Spirlet, M. R.; Rebizant, J.; Apostolidis, C.; Kanellakopulos, B. *Acta Crystallogr*. **1992**, *C48*, 2135.

contrast, attempts to synthesize a U(IV)−dzni complex were not successful. The difficulties associated with isolating a U(IV)−dzni compound may be due to the increased Lewis acidity and oxophilicity of U(IV) relative to Zr(IV). Ligand redistribution pathways appear to be possible in the presence of U(IV) such that compounds such as **3** can form.

Acknowledgment. This research was supported by the Division of Chemical Sciences of the Office of Basic Energy Sciences of the Department of Energy. We thank Dr. Matthew A. Johnston for X-ray crystallographic assistance and Dr. Noémia Marques for helpful suggestions.

Supporting Information Available: Crystallographic data for **1**−**3** in CIF format. This material is available free of charge via the Internet at http://pubs.acs.org.

IC010703X